Mon. Not. R. astr. Soc. (1988) **232,** 131–145

Photoelectric and electronographic photometry of the globular cluster NGC 1851

Ram Sagar,* R. D. Cannon† and M. R. S. Hawkins
Royal Observatory, Blackford Hill, Edinburgh EH9 3HJ

Accepted 1987 November 2. Received 1987 October 30; in original form 1987 April 22

Summary. The colour–magnitude diagram for NGC 1851 is presented to a limit of $V=21.0$ mag, approximately 2 mag below the main-sequence turn-off point, on the basis of *UBV* photoelectric photometry and electronographic *BV* photometry. The main-sequence turn-off parameters are $(B-V)_t=0.40\pm0.03$ mag; $V_t=19.45\pm0.1$ mag. From the location of the horizontal branch stars, the apparent distance modulus to the cluster has been estimated as 15.45 ± 0.2 mag. An age of 15 ± 3 Gyr has been assigned to the cluster from the fitting of Vanden-Berg & Bell theoretical isochrones.

1 Introduction

In order to establish whether or not globular clusters were formed during the collapse of the protogalaxy it is necessary to establish whether they all have almost the same age and primordial helium abundance (Eggen, Lynden-Bell & Sandage 1962; Searle & Zinn 1978). This involves obtaining colour–magnitude diagrams (CMDs) below the location of the main-sequence turn-off point, and chemical abundances of stars for as many globular clusters as possible. To achieve these aims, a considerable observational effort has been made during the last few years, but no photometric study to the turn-off point of the relatively nearby cluster NGC 1851 has been made. NGC 1851 is particularly well suited for this type of work because it is a populous cluster in an uncrowded field with low reddening. The present work gives a first determination of the main-sequence turn-off point, using photoelectric and electronographic data. These data were obtained just prior to the widespread introduction of CCD cameras for this type of work; although they are of lower accuracy than the best CCD data, they do serve to determine the location of the main-sequence and to show that the age of NGC 1851 is consistent with that of other globular clusters.

2 Previous work on NGC 1851

The southern globular cluster NGC 1851 (CO 512−400) has been investigated a number of times photometrically and spectroscopically; Stetson (1981) has discussed in detail existing earlier work

*Present address: Indian Institute of Astrophysics, Bangalore 560 034, India.
†Present address: Anglo-Australian Observatory, PO Box 296, Epping, NSW 2121, Australia.

on the cluster. Kinman (1959) and Harris & Racine (1979) indicated that NGC 1851 is a moderately metal-poor cluster, and Zinn & West (1984) give [Fe/H] = −1.36 on a scale where [Fe/H] = −0.71 for 47 Tuc, −1.40 for M5, −1.54 for NGC 6752 and −1.69 for M3. Recently Hesser *et al.* (1982) have published spectroscopic observations of 18 stars in NGC 1851 and found that 3 out of 8 bright red giants possess extremely strong CN bands at the wavelengths 3883 and 4216 Å. Variables in the cluster region have been studied by Liller (1975) and Wehlau *et al.* (1978, 1982). The cluster contains 22 RR Lyrae variables, enough for useful comparison with the relatively small number of RR Lyrae-rich clusters. Various photometric studies by Alcaino (1969, 1971, 1976) indicate values ranging from 0.10 to 0.34 mag for the reddening $E(B-V)$, and from 15.15 to 15.50 mag for the apparent distance modulus $(m-M)$. Stetson (1981) has published a CMD based on a large sample of stars brighter than $V \approx 18$ mag. He gives a low value of reddening, $E(B-V) = 0.02 \pm 0.02$ mag and a distance modulus, $(m-M)_0 = 15.39 \pm 0.23$ mag. He points out that the cluster CMD is normal for its metal abundance although the distribution of stars on the horizontal branch is slightly peculiar in the sense that it covers a wide range of colours and has a distribution with peaks towards either end of the observed colour range. The main motivation for making a new CMD was that none of these studies went faint enough to reach below the main-sequence turn-off point.

3 Observations and reductions

The observations obtained for the construction of the CMD can be divided into two groups, the *UBV* photoelectric photometry and the *BV* electronographic measures.

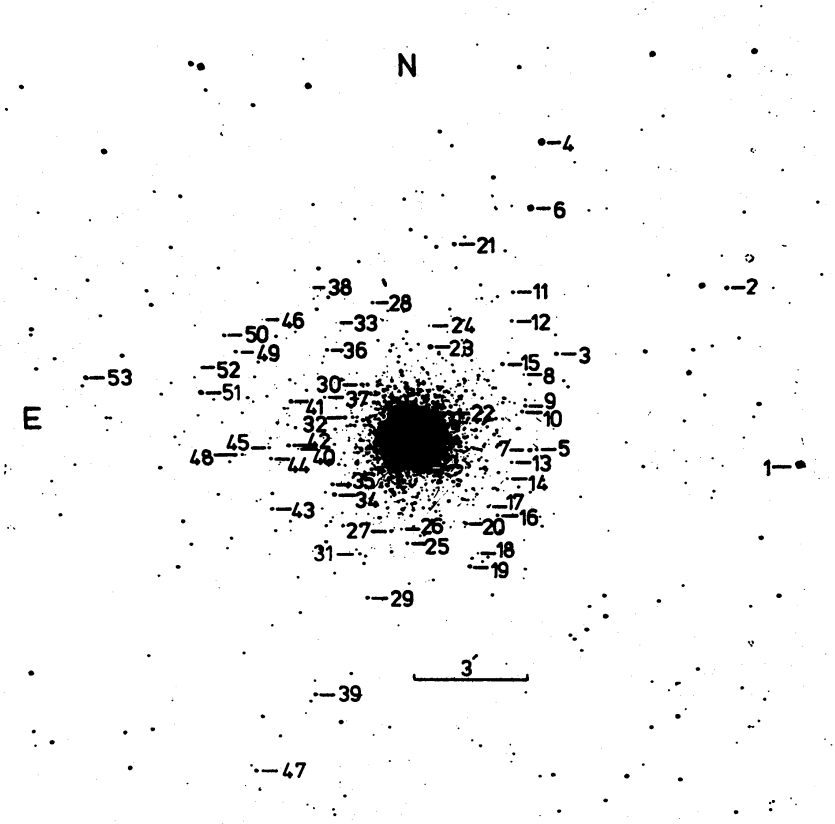

Figure 1. Identification chart for photoelectrically observed stars. This and Fig. 2 are reproduced from a 45-min photographic *V* plate taken with the 3.9-m AAT.

3.1 *UBV* PHOTOELECTRIC PHOTOMETRY

Fifty-three stars in the cluster region were observed photoelectrically in the *UBV* system between 1970 December to 1972 May, as part of a series which was intended to provide a homogeneous set of broadband photometric data for several of the closest southern globular clusters. The observations were made using standard 2-channel and 1-channel photoelectric photometers on the Australian National University's 1-m and 0.4-m telescopes at Siding Spring Observatory. The observations of faint cluster stars were tied each night to a set of local standards near the clusters, and these in turn were tied to Cousins' (1973) E-region standards on the best photometric nights. Further details of the equipment, observing procedures and accuracy of the data for stars with $V<16$ mag are as described by Cannon & Stobie (1973) for ω Centauri. For stars with $V\geqslant 16$ mag, the details of the observing procedure and photometric accuracy are as described by Cannon (1981). The observed stars are identified in Fig. 1 and their *UBV* photoelectric data are listed in Table 1.

Stetson (1981), on the basis of 18 common stars between his photometry and the present,

Table 1. *UBV* photoelectric photometry for stars in NGC 1851.

Star	V (mag)	(B-V) (mag)	(U-B) (mag)	n	t	Remarks	Star	V (mag)	(B-V) (mag)	(U-B) (mag)	n	t	Remarks
1	9.56	1.05	0.91	8		std	31	16.39	0.06	0.14	1	50	
2	13.96	1.04	0.68	1			32	14.35	1.17	-	1		
3	13.41	1.68	1.98	2			33	18.33	0.76	-	1	200	
4	11.44	0.56	0.05	8		std	34	13.21	1.67	1.51:	2*		
5	15.47	1.02	0.93	1			35	14.35	1.14	0.89:	2*		
6	11.73	0.59	0.01	8		std	36	14.92	1.11	0.75	1		
7	13.40	1.58	1.51:	2*			37	16.87	0.00	-0.16	2*	100	
8	17.26	0.84	-	1	50		38	18.34	0.83	-	1	200	
9	14.91	0.85	0.43	2			39	14.34	0.95	-	1		
10	14.82	1.17	0.91	2			40	17.24	0.74	-	2	75	
11	15.16	0.86	0.24	2			41	13.59	1.44	1.49	2		
12	15.60	0.62	0.03	2			42	13.80	1.48	1.40:	2		
13	16.22	0.61	-	2	60		43	14.51	1.22	1.31	1		
14	16.80	0.94	-	2	100		44	14.87	1.04	0.90:	2*		
15	14.04	1.28	1.34	2			45	15.87	0.23	0.14	1		
16	15.35	0.99	0.71	3*			46	17.95	0.68	-	1	100	
17	15.80	0.94	0.38:	3*			47	13.42	1.54	1.73	1		
18	17.25	0.67	-	1	50		48	16.78	0.05	-0.07	1	25	
19	14.27	0.55	0.05	1			49	14.91	0.83	0.58:	2*		
20	14.49:	0.88:	0.47:	1		double	50	14.97	0.72	0.05:	2*		
21	13.52	1.58	1.77	2			51	13.18	0.73	0.24	2		
22	13.16	1.62	1.10	1			52	18.49	0.43	-	1	200	
23	13.28	0.72	0.15	2			53	13.83	1.79	2.15	1		
24	17.01	0.76	-	2	75								
25	15.88	0.87	-	1									
26	17.22	0.86:	-	2	150								
27	16.57	0.02	-0.21:	2*	100								
28	16.10	0.16	0.16	2	100								
29	14.66	0.73	0.05	1									
30	14.22	1.27	0.85	1									

Column 5 gives n, the number of nights of observations. In the case of local standards (std), n is the number of nights used in the tie-in to *UBV* standards. An asterisk indicates one less U observation. t is the integration time in seconds for stars with $V\geqslant 16$.

concluded that the two sets of photometric observations agreed very well. Twenty stars in common between the present photometry and Alcaino's early (1969) photometry yield $\Delta V = -0.11 \pm 0.06$ mag, $\Delta(B-V) = -0.09 \pm 0.07$ mag, $\Delta(U-B) = -0.10 \pm 0.11$ mag in the sense (present – Alcaino), which are very large differences in comparison with the quoted photometric errors. However, Alcaino (1976) himself later found similar offsets compared with his 1969 data. The present photometry has only four stars common with his photometry, which yield $\Delta V = 0.01 \pm 0.03$ mag and $\Delta(B-V) = 0.015 \pm 0.019$ mag.

3.2 *BV* ELECTRONOGRAPHIC PHOTOMETRY

The electronographic observations for NGC 1851 were carried out with the 1.5-m Danish Telescope at La Silla, Chile in 1979 November and 1981 October, using the 8-cm McMullan electronographic camera and Ilford L4 emulsion. The details of the observational material are given in Table 2. In addition, a number of flat field exposures were obtained on the twilight sky during each observing run. The electronographic films were scanned on the RGO PDS microdensitometer using the techniques described by Penny (1984). The higher precision and measuring speed of this machine and automatic nature of its operation make it a useful tool for photometric studies of large numbers of stars. For the flat field exposures, a scan speed of 23.5 mm s^{-1} and a 24 μm^2 measuring aperture were used with 20 μm steps. The measured scan area in a 2048×2048 raster was chosen in such a way that it covered the entire cluster field under investigation. For the reasons mentioned by Penny (1984), the NGC 1851 exposures were scanned at a slower speed of 5 mm s^{-1} with an 11 μm^2 measuring aperture using 10 μm steps. For NGC 1851 itself, 10 areas (marked R1–R10 in Fig. 2) of 512×512 raster size were scanned. The areas were chosen in such a way that each contained a few photoelectric standards and also were situated in regions which were neither overcrowded nor located very far from the cluster centre and hence have not included appreciable numbers of field stars. In order to measure the clear film level and to check on zero-point drift during measurement, the scan was made in the MULTI SEGMENTED mode of the PDS. In this mode, the scan was automatically interrupted 16 times for flat field exposures and 4 times for cluster exposures in order to perform a 30×30 raster on a reference area of the film which was exposed to cathode background flux, but not to the sky. The STARLINK programs written by Penny were used to convert the raw PDS measures into images with pixel values linearly related to the incident photon flux. The methods used in the above programs have been described briefly by Penny (1984). PDS scans for the flat fields were also reduced in the same way, and were then smoothed. The NGC 1851 exposures were then divided by these flat fields. During

Table 2. Electronographic film data of NGC 1851.

Film	Exposure (min)	Filter	Date
25.7.8	55	*B*	1979 November 21
25.7.9	45	*V*	1979 November 21
25.7.10	1	*B*	1979 November 21
25.7.11	1	*V*	1979 November 21
25.8.12	10	*B*	1979 November 22
25.8.13	10	*V*	1979 November 22
25.8.14	20	*B*	1979 November 22
25.9.10	20	*V*	1979 November 23
27.8.8	60	*B*	1981 October 27
27.8.9	60	*V*	1981 October 27

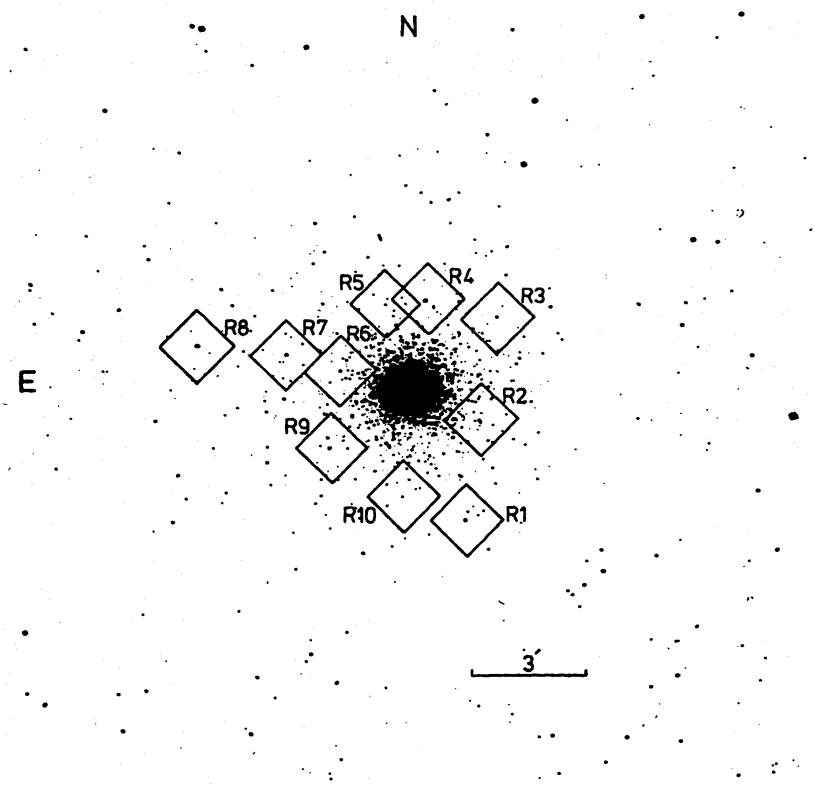

Figure 2. Identification chart for the regions R1–R10 scanned using PDS on the electronographic film.

the above processes, the alignment of the various films was made, using three cathode fiducial marks. The B and V flat fields show maximum overall variations of less than 10 per cent.

The star magnitudes were estimated by profile fitting. By means of a 2-dimensional iterative linearized least-squares analysis, stars on each exposure were fitted with a 2D Lorentz profile. We have also applied a small correction to the PDS magnitudes, described in detail by Penny (1984). The colour equation of the camera was determined from the stars observed by Stetson (1981). For this purpose stars brighter than $V=15.0$ mag were used because for fainter stars the photometric errors are relatively large. For these stars electronographic magnitudes are estimated from the 1 and 10 min exposures. $(V-V_{eg})$ versus $(B-V)$ and $(B-B_{eg})$ versus $(B-V)$ are plotted in Fig. 3 and a least-squares straight-line fit is also shown, where the subscript 'eg' refers to electronographic

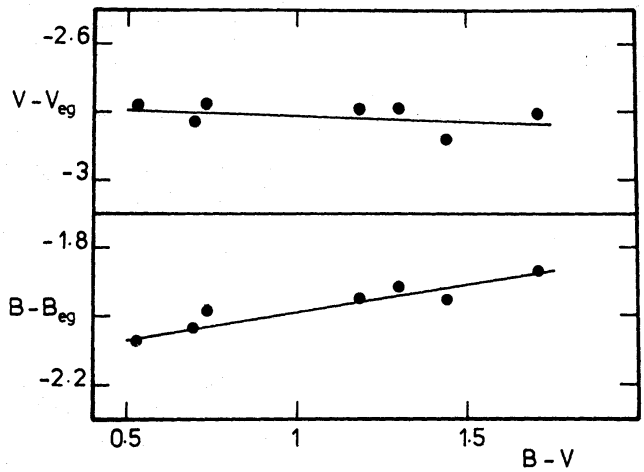

Figure 3. Plot of $(V-V_{eg})$ versus $(B-V)$ and $(B-B_{eg})$ versus $(B-V)$. Solid lines represent the best-fit straight lines using least-squares solutions.

Table 3. Electronographic *BV* magnitudes and positions of stars measured in NGC 1851. Positions are with respect to star 3 in Fig. 1. $\Delta\alpha$ and $\Delta\delta$ in arcsec are the difference in right ascension and declination respectively. N_v and N_b are number of measurements in *V* and *B* filters respectively.

Star	Δα	Δδ	V (mag)	B-V (mag)	N_v	N_b	Star number Stet-son	Fig. 1
			Region 1					
1	147	-368	20.31	0.54	3	2		
2	162	-364	20.70	0.71	2	2		
3	155	-374	19.82	0.57	3	2		
4	157	-373	20.08	0.57	3	3		
5	161	-377	20.90	0.83	2	3		
6	175	-372	19.19	0.60	3	3		
7	158	-386	19.96	0.59	2	2		
8	165	-389	19.58	0.61	3	2		
9	188	-365	16.13	0.78	2	2	242	
10	176	-357	16.21	0.65	4	4	243	
11	180	-343	19.94	0.60	3	3		
12	187	-349	20.10	0.86	2	2		
13	189	-350	20.67	1.10	2	2		
14	198	-349	17.15	0.69	2	3	239	18
15	202	-347	20.19	0.73	3	2		
16	205	-334	20.45	0.72	3	2		
17	198	-335	20.51	0.60	2	3		
18	205	-329	19.32	0.65	3	3		
19	208	-320	19.73	0.61	3	2		
20	216	-324	18.93	0.63	3	2		
21	219	-327	19.63	0.64	2	3		
22	212	-327	21.04	0.61	2	3		
23	211	-333	20.49	0.89	2	3		
24	214	-337	20.51	0.78	2	2		
25	212	-346	20.91	0.94	3	2		
26	221	-335	20.71	0.82	2	2		
27	222	-330	20.69	0.84	3	2		
28	227	-328	20.73	0.56	3	2		
29	230	-327	20.80	0.50	3	2		
30	231	-324	20.58	0.50	2	2		
31	224	-343	20.11	0.64	3	2		
32	245	-342	18.87	0.69	3	3		
33	251	-342	18.99	0.63	2	2		
34	232	-353	21.08	0.81	2	3		
35	232	-358	20.67	0.65	2	3		
36	223	-357	19.95	0.61	3	3		
37	224	-348	21.17	0.98	2	2		
38	212	-358	16.18	0.47	5	4	240	
39	208	-35.	19.81	0.54	2	2		
40	204	-359	19.99	0.69	3	3		
41	218	-372	14.30	0.56	2	2	241	19
42	216	-384	20.55	0.83	2	2		
43	226	-394	19.45	0.60	3	3		
44	222	-394	20.60	0.88	3	3		
45	212	-402	20.76	0.77	2	3		
46	202	-402	20.88	0.80	2	3		
47	204	-408	19.49	0.67	3	3		
48	190	-411	20.38	0.51	3	2		
49	200	-414	20.00	0.56	3	2		
50	207	-418	19.47	0.60	2	3		
51	211	-422	20.80	0.71	3	3		
52	218	-431	19.51	0.60	2	2		
53	236	-424	20.03	0.78	3	2		
54	235	-409	19.14	0.59	3	3		
55	268	-396	19.83	0.64	2	2		
56	260	-389	20.38	0.61	2	3		
57	255	-392	19.72	0.60	2	3		
58	245	-396	20.14	0.67	3	3		
59	242	-386	21.04	0.56	2	2		
60	238	-387	19.98	0.54	3	2		
61	229	-387	20.94	0.72	3	2		
62	238	-378	19.99	0.64	3	2		
63	242	-376	20.88	0.72	2	3		
64	235	-366	19.79	0.57	3	2		
65	242	-367	19.31	0.67	3	3		
66	250	-375	19.52	0.65	3	2		
67	249	-378	20.78	0.65	3	2		
68	258	-355	20.79	0.92	2	2		
69	264	-357	19.74	0.53	3	2		
70	268	-356	20.46	0.71	2	2		
71	272	-355	18.85	0.68	3	3		
72	274	-360	20.66	0.51	2	3		
73	276	-363	21.00	0.72	2	2		
74	269	-371	20.51	0.71	3	2		
75	278	-385	18.74	0.85	3	3		
76	289	-373	20.43	0.45	3	2		
77	284	-370	20.37	0.69	2	2		
78	258	-407	19.95	0.61	2	2		
			Region 2					
1	112	-188	16.22	0.54	4	3	295	13
2	114	-191	18.93	0.54	3	3		
3	119	-185	19.78	0.83	2	2		
4	108	-208	18.68	0.67	2	2		
5	118	-207	19.04	0.46	3	3		
6	120	-204	19.08	0.41	3	3		
7	124	-204	18.08	0.77	1	2		
8	125	-200	19.12	0.52	3	3		
9	134	-196	19.43	0.59	3	2		
10	129	-185	19.33	0.60	3	3		
11	130	-183	18.47	0.69	3	3		
12	153	-152	19.19	0.52	2	2		
13	157	-152	19.59	0.57	2	2		
14	163	-144	19.60	0.78	3	2		
15	173	-140	19.06	0.65	3	2		
16	173	-143	19.13	0.70	3	3		
17	181	-143	19.24	0.59	2	2		
18	185	-149	19.19	0.54	3	2		
19	171	-154	16.41	0.82	2	2	299	
20	164	-152	19.38	0.58	2	2		
21	174	-158	16.11	0.55	2	2	300	
22	164	-169	19.41	0.52	3	3		
23	159	-160	20.11	0.36	3	3		
24	157	-162	19.44	0.57	2	2		
25	154	-164	19.01	0.66	2	2		
26	151	-171	19.67	0.52	3	2		
27	155	-172	19.85	0.39	2	2		
28	149	-175	19.76	0.42	3	2		
29	151	-179	19.10	0.56	3	3		
30	159	-184	19.66	0.35	3	2		
31	154	-186	19.23	0.36	2	2		
32	151	-188	19.02	0.60	2	2		
33	152	-191	19.49	0.57	2	2		
34	143	-194	18.63	0.75	3	3		
35	144	-195	19.66	0.42	3	2		
36	140	-200	18.46	0.70	2	2		
37	144	-200	20.13	0.71	3	2		
38	143	-205	16.71	-0.05	3	2	282	
39	151	-207	16.25	0.82	2	3		
40	148	-208	19.79	0.40	3	2		
41	139	-208	19.76	0.53	3	2		
42	140	-213	19.57	0.33	3	2		
43	135	-219	19.92	0.46	3	2		
44	134	-223	19.32	0.52	3	3		
45	143	-217	19.25	0.50	3	2		
46	147	-215	19.44	0.46	3	2		
47	151	-215	19.12	0.42	2	2		
48	152	-212	19.18	0.48	3	2		
49	162	-211	18.66	0.59	3	3		
50	157	-233	16.10	0.63	2	2	268	
51	152	-232	17.20	1.60	2	2	267	
52	147	-236	16.08	0.65	2	2	266	
53	154	-238	19.54	0.51	3	2		
54	173	-230	18.59	0.49	3	2		
55	174	-219	19.05	0.41	2	2		
56	180	-221	18.96	0.59	3	3		
57	179	-216	19.88	0.44	2	2		
58	178	-213	17.26	0.73	4	3	269	
59	177	-207	18.59	0.72	2	3		
60	173	-206	17.24	0.79	3	2	281	
61	180	-203	19.04	0.45	3	2		
62	184	-197	16.71	0.78	3	3	278	
63	175	-196	14.18	1.07	2	2	279	
64	158	-198	19.33	0.47	2	3		
65	179	-177	18.64	0.43	2	3		
66	186	-179	18.73	0.53	3	3		
67	186	-182	17.01	-0.09	3	2	277	
68	180	-164	16.06	0.81	2	2	301	
69	189	-163	16.17	0.57	2	2	302	
70	191	-167	20.06	0.54	2	2		
71	190	-174	19.18	0.44	3	2		
72	197	-176	18.68	0.62	3	2		
73	199	-180	18.98	0.58	2	2		
74	195	-197	19.30	0.54	3	3		
75	200	-203	19.63	0.83	3	2		
76	204	-206	18.58	0.71	3	3		
77	211	-222	19.16	0.43	3	3		
78	202	-233	15.59	0.98	2	2	264	
79	202	-240	18.95	0.68	3	2		
80	195	-243	16.04	0.83	2	2	265	
81	192	-231	18.67	0.64	3	2		
82	181	-226	18.86	0.46	3	3		
83	169	-228	19.53	0.31	3	3		
84	123	-216	16.84	0.80	3	3	283	14
85	159	-245	19.13	0.51	2	2		
86	164	-248	19.86	0.40	2	2		
87	179	-254	19.65	0.63	2	3		
			Region 3					
1	60	1	19.65	0.73	2	2		
2	61	- 4	20.23	0.50	2	2		
3	62	- 3	20.35	0.57	2	2		
4	66	- 2	20.08	0.70	2	2		
5	71	- 6	20.17	0.74	2	2		
6	73	- 8	20.07	0.58	2	3		
7	80	- 6	20.39	0.32	2	3		
8	78	- 16	20.38	0.71	3	3		
9	70	- 21	20.82	0.40	3	3		
10	59	- 16	20.08	0.43	2	2		
11	66	- 33	20.37	0.68	2	2		

Table 3–*continued*

Star	Δα	Δδ	V (mag)	B–V (mag)	N_v	N_b	Star number Stetson	Star number Fig. 1
12	68	−32	20.52	0.56	2	3		
13	75	−34	17.18	0.86	3	3	328	8
14	78	−28	19.83	0.51	2	2		
15	79	−26	19.68	0.58	2	3		
16	87	−25	19.49	0.57	2	2		
17	106	−35	18.70	0.71	4	4		
18	98	−43	19.94	0.50	3	3		
19	99	−47	20.43	0.67	3	2		
20	98	−53	19.73	0.59	3	2		
21	106	−54	18.95	0.67	2	2		
22	109	−55	19.42	0.57	2	2		
23	107	−58	19.19	0.53	3	2		
24	111	−58	19.30	0.54	3	2		
25	111	−51	18.96	0.58	3	2		
26	111	−48	19.87	0.67	3	2		
27	115	−36	18.90	0.53	3	2		
28	116	−32	20.29	0.64	3	3		
29	119	−35	20.29	0.55	2	2		
30	122	−36	19.89	0.36	2	2		
31	120	−29	20.88	0.41	2	2		
32	122	−14	13.99	1.31	2	2	333	15
33	130	−4	20.36	0.43	3	3		
34	124	−5	19.66	0.50	2	2		
35	124	−3	19.37	0.47	2	2		
36	113	1	20.58	0.78	3	2		
37	109	−3	20.66	0.62	2	3		
38	106	−12	19.85	0.55	2	2		
39	96	−13	19.92	0.59	2	2		
40	96	−6	20.74	0.53	3	3		
41	100	−7	20.55	0.54	3	3		
42	108	5	16.85	0.89	2	3	332	
43	100	16	19.34	0.60	3	3		
44	113	24	19.39	0.49	3	3		
45	104	30	19.30	0.51	3	2		
46	78	16	20.19	0.66	2	2		
47	96	28	20.54	0.42	2	2		
48	98	31	17.75	0.79	3	2	331	
49	99	34	19.53	0.45	3	2		
50	108	41	19.53	0.51	2	2		
51	109	39	20.29	0.53	3	2		
52	115	43	20.20	0.43	3	2		
53	127	42	18.68	0.73	2	2		
54	124	40	19.10	0.52	2	2		
55	120	32	19.74	0.64	2	3		
56	139	29	19.91	0.49	3	3		
57	153	25	20.41	0.43	3	2		
58	144	15	20.09	0.53	3	3		
59	131	2	20.16	0.81	3	3		
60	143	2	20.34	0.60	3	2		
61	150	−1	19.35	0.55	3	2		
62	160	0	19.21	0.55	3	2		
63	163	10	19.77	0.61	2	3		
64	174	−3	19.20	0.62	3	3		
65	181	−4	18.28	0.85	2	3		
66	179	−9	19.31	0.61	2	3		
67	175	−10	20.17	0.52	2	2		
68	161	−12	19.86	0.50	3	2		
69	153	−10	20.00	0.59	2	2		
70	152	−16	18.84	0.68	3	2		
71	143	−17	19.57	0.68	3	2		
72	144	−26	17.48	0.70	4	4	334	
73	144	−34	20.02	1.07	2	2		
74	140	−31	20.45	0.80	3	3		
75	134	−31	20.15	0.66	3	2		
			Region 4					
1	267	73	20.58	0.61	2	2		
2	257	66	19.77	0.56	3	3		
3	258	58	18.00	0.78	3	2	391	
4	243	46	17.64	0.81	3	3	390	
5	249	45	18.83	0.63	3	3		
6	252	44	19.45	0.52	3	3		
7	252	41	20.41	0.59	3	3		
8	236	41	19.91	0.38	3	3		
9	233	36	20.08	0.52	3	2		
10	243	34	20.42	0.68	2	2		
11	238	32	19.83	0.57	3	2		
12	234	23	20.16	0.54	2	2		
13	233	23	19.84	0.38	2	3		
14	230	24	19.83	0.48	3	3		
15	228	22	19.86	0.53	2	2		
16	220	22	19.79	0.46	3	3		
17	229	8	19.55	0.26	3	3		
18	233	13	20.39	0.43	3	2		
19	237	7	19.30	0.42	2	3		
20	246	5	19.46	0.47	3	3		
21	262	25	19.16	0.36	2	2		
22	261	29	18.95	0.53	2	3		
23	267	27	19.83	0.49	2	2		
24	269	25	20.75	0.24	2	2		
25	266	21	20.21	0.52	2	2		
26	283	21	13.34	0.68	2	2	401	23
27	286	32	19.78	0.37	2	2		
28	291	37	19.02	0.54	3	3		
29	287	43	18.53	0.69	3	3		
30	277	40	20.45	0.42	2	2		
31	269	50	19.31	0.43	3	3		
32	277	60	19.42	0.64	3	3		
33	284	58	17.18	0.77	3	4	400	24
34	295	48	19.62	0.46	3	3		
35	303	36	18.89	0.40	3	2		
36	313	35	19.49	0.37	3	3		
37	318	37	19.57	0.46	2	2		
38	321	39	18.54	0.64	2	3		
39	[illegible]	40	20.28	[illegible]	[illegible]	2		
40	325	40	19.87	0.42	2	2		
41	327	37	19.87	0.45	4	2		
42	333	38	19.62	0.39	4	3		
43	320	31	19.02	0.44	5	5		
44	310	26	16.25	0.89	3	4		10
45	302	22	19.77	0.40	4	3		
46	307	21	19.85	0.37	5	4		
47	311	22	19.33	0.42	3	2		
48	306	17	19.60	0.41	3	3		
49	320	24	20.05	0.43	4	3		
50	343	36	16.75	0.94	5	5		12
51	340	26	18.63	0.67	5	4		
52	336	27	16.24	0.93	5	5		11
53	344	21	19.71	0.41	3	3		
54	352	15	19.36	0.55	4	5		
55	347	14	19.06	0.54	4	3		
56	345	9	19.81	0.44	2	4		
57	342	9	19.05	0.49	4	2		
58	344	5	19.85	0.28	2	2		
59	341	6	20.28	0.31	3	2		
60	335	1	19.55	0.34	4	4		
61	329	12	19.94	0.37	2	2		
62	328	16	16.20	0.41	6	5		9
63	323	11	19.58	0.35	4	5		
64	321	4	19.26	0.30	3	2		
65	319	1	19.67	0.26	4	3		
66	307	11	19.32	0.32	2	3		
67	305	9	19.68	0.32	2	2		
68	313	−4	17.93	0.71	3	2		
69	293	1	18.40	0.44	2	3		
70	292	−1	19.10	0.45	3	2		
71	285	4	18.88	0.55	3	2		
72	285	−1	19.69	0.39	3	3		
73	276	−1	19.52	0.23	3	3		
74	285	−15	19.14	0.46	3	3		
75	281	−12	18.57	0.25	3	3		
76	278	−9	17.92	0.57	3	3		
77	271	−10	18.41	0.58	3	2		
78	262	−17	19.11	0.32	3	3		
79	264	−7	18.19	0.68	4	3		
80	264	−1	18.94	0.43	3	3		
81	258	0	17.01	0.80	5	4	404	
82	250	0	19.63	0.39	2	2		
83	250	−4	17.36	0.76	5	4	405	
84	257	−8	19.79	0.25	3	3		
85	272	−13	19.71	0.33	3	3		
			Region 5					
1	378	69	18.33	0.65	2	2		
2	372	64	18.50	0.66	2	2		
3	363	64	20.38	0.52	2	2		
4	360	60	18.83	0.57	2	2		
5	361	52	20.02	0.60	2	2		
6	353	53	20.35	0.35	2	2		
7	349	53	19.78	0.46	2	2		
8	343	55	20.03	0.36	2	2		
9	338	51	18.43	0.67	2	2		
10	335	49	16.56	0.72	2	2		13
11	333	46	18.79	0.62	2	2		
12	301	9	20.62	0.23	2	2		
13	311	8	20.70	0.22	2	2		
14	336	31	20.02	0.34	2	2		
15	347	37	19.90	0.32	2	2		
16	359	33	19.46	0.36	2	2		
17	365	44	20.31	0.37	2	2		
18	370	44	20.41	0.45	2	2		
19	375	48	19.06	0.42	2	2		
20	380	46	20.92	0.57	2	2		
21	373	56	19.94	0.48	2	2		
22	381	58	19.10	0.43	2	2		
23	382	54	19.36	0.55	2	2		
24	391	56	20.33	0.41	2	2		
25	384	48	20.22	0.48	2	2		
26	388	47	19.11	0.51	2	2		
27	404	53	20.23	0.39	2	2		
28	419	45	19.41	0.34	2	2		
29	414	44	19.35	0.41	2	2		
30	399	45	19.21	0.43	2	2		
31	390	41	19.90	0.54	2	2		
32	390	36	19.22	0.48	2	2		
33	403	39	20.38	0.39	2	2		
34	401	35	16.19	0.94	2	2		35
35	393	28	19.34	0.41	2	2		
36	386	26	19.58	0.37	2	2		
37	384	24	19.34	0.52	2	2		
38	371	23	18.12	0.73	2	2		
39	369	27	16.70	0.86	2	2		8
40	364	26	18.83	0.43	2	2		
41	342	0	18.57	0.68	2	2		
42	358	−4	16.71	0.11	2	2		5
43	364	0	19.75	0.50	2	2		
44	369	−4	20.16	0.32	2	2		
45	366	−29	19.11	0.46	2	2		
46	376	−25	19.32	0.51	2	2		
47	378	−18	19.49	0.48	2	2		
48	383	−11	18.47	0.40	2	2		
49	388	−12	19.55	0.36	2	2		
50	397	0	19.49	0.41	2	2		
51	389	17	20.21	0.51	2	2		
52	403	25	19.28	0.40	2	2		
53	407	19	19.26	0.39	2	2		
54	408	16	20.22	0.51	2	2		
55	420	39	18.92	0.57	2	2		
56	426	35	20.10	0.35	2	2		
57	[illegible]	[illegible]	[illegible]	[illegible]	[illegible]	2		

Table 3–*continued*

Star	Δα	Δδ	V (mag)	B-V (mag)	N_v	N_b	Star number Stet-son	Fig. 1
58	427	28	19.87	0.46	2	2		
59	436	26	19.24	0.44	2	2		
60	448	21	19.27	0.50	2	2		
61	446	19	19.99	0.38	2	2		
62	450	14	20.14	0.45	2	2		
63	435	19	20.21	0.37	2	2		
64	428	20	19.73	0.43	2	2		
65	426	15	20.12	0.47	2	2		
66	425	13	20.05	0.30	2	2		
67	441	8	18.93	0.39	2	2		
68	438	5	18.36	0.27	2	2		
69	430	6	19.84	0.25	2	2		
70	428	2	19.12	0.37	2	2		
71	429	- 6	19.75	0.50	2	2		
72	412	- 10	20.14	0.37	2	2		
73	414	- 4	19.76	0.29	2	2		
74	412	0	19.30	0.38	2	2		
75	409	- 3	19.34	0.39	2	2		
76	402	- 3	19.14	0.41	2	2		
77	405	- 16	19.06	0.43	2	2		
78	406	- 19	19.36	0.46	2	2		
79	404	- 25	18.96	0.58	2	2		
			Region 6					
1	478	- 47	18.94	0.56	3	2		
2	481	- 51	18.01	0.72	3	3		
3	489	- 42	19.53	0.56	2	2		
4	493	- 48	19.21	0.62	3	2		
5	484	- 58	19.84	0.84	3	2		
6	478	- 63	18.93	0.67	3	3		
7	477	- 60	19.52	0.38	2	3		
8	471	- 55	17.53	0.71	3	3		
9	466	- 53	19.05	0.49	3	3		
10	463	- 60	19.75	0.57	3	3		
11	469	- 60	19.52	0.58	2	2		
12	462	- 76	16.14	0.96	2	2	75	
13	441	- 81	18.78	0.47	3	2		
14	437	- 88	18.52	0.64	3	3		
15	446	- 88	18.59	0.44	2	2		
16	445	-105	14.43	1.28	2	2	129	
17	442	-114	16.03	0.66	2	2		
18	454	-123	18.18	0.76	3	3		
19	464	-114	16.36	0.05	2	2	131	
20	459	-107	15.88	0.96	3	3	130	
21	458	-100	16.43	0.80	2	2	128	
22	455	- 98	18.99	0.49	3	3		
23	462	- 92	19.50	0.38	3	2		
24	466	- 90	19.05	0.44	2	2		
25	467	- 92	18.81	0.63	3	2		
26	470	- 92	17.62	0.81	2	2		
27	470	- 81	15.64	0.50	2	2		
28	488	- 80	19.34	0.59	2	3		
29	480	- 69	19.94	0.37	2	3		
30	487	- 69	19.01	0.55	3	3		
31	485	- 64	19.30	0.43	3	3		
32	489	- 63	18.23	0.60	2	3		
33	489	- 60	19.21	0.45	3	3		
34	494	- 61	20.05	0.38	3	3		
35	497	- 62	19.21	0.36	2	2		
36	503	- 59	19.46	0.37	3	3		
37	505	- 66	19.09	0.47	2	3		
38	503	- 68	17.88	0.70	3	3		
39	509	- 66	19.80	0.56	3	3		
40	518	- 66	19.26	0.50	3	3		
41	510	- 70	19.28	0.36	3	3		
42	508	- 73	19.51	0.49	3	3		
43	503	- 73	19.52	0.45	2	2		
44	505	- 79	19.13	0.20	2	3		
45	505	- 82	17.27	0.73	5	4	78	
46	500	- 86	18.56	0.59	3	2		
47	496	- 85	19.91	0.51	2	2		
48	478	- 78	16.04	0.67	2	2	76	
49	483	- 81	20.01	0.57	2	2		
50	498	- 95	18.06	0.64	3	3		
51	486	- 99	14.35	1.21	2	2	126	32
52	468	- 99	16.08	0.60	2	2	127	
53	471	-102	18.49	0.56	3	2		
54	469	-107	18.91	0.42	3	2		
55	482	-115	16.03	0.85	2	2	133	
56	468	-124	19.36	0.47	2	3		
57	471	-144	18.91	0.49	3	2		
58	478	-141	17.47	0.71	3	2		
59	478	-135	17.88	0.79	3	2		
60	492	-121	18.06	0.70	2	2		
61	491	-113	19.02	0.70	2	3		
62	497	-117	18.85	0.77	3	3		
63	501	-119	18.78	0.55	3	2		
64	505	-126	17.83	0.75	3	3		
65	510	-120	16.18	0.83	2	2	123	
66	520	-116	19.59	0.49	3	3		
67	529	-108	16.91	0.84	3	3		
68	534	-104	19.42	0.43	3	3		
69	529	-103	19.53	0.40	3	3		
70	531	- 98	19.02	0.52	3	3		
71	531	- 94	18.67	0.73	2	2		
72	525	- 96	19.08	0.49	2	3		
73	522	- 99	18.57	0.42	3	2		
74	509	-102	19.18	0.48	3	3		
75	508	-100	19.17	0.37	3	3		
76	525	- 74	18.92	0.53	3	3		
77	536	- 76	19.58	0.44	3	3		
78	537	- 79	19.67	0.46	3	3		
79	535	- 86	19.38	0.39	2	2		
80	543	- 90	19.99	0.37	3	3		
81	550	-102	19.59	0.38	3	2		
82	545	-114	17.56	0.75	2	2		
83	538	-119	17.95	0.74	2	2		
84	534	-121	19.90	0.52	2	2		
85	541	-104	20.20	0.48	2	2		
86	537	-108	19.89	0.40	2	2		
87	532	-114	19.57	0.66	2	2		
88	531	-116	17.71	0.71	2	2		
89	495	-132	20.00	0.45	2	2		
90	485	-138	19.13	0.37	3	2		
91	489	-139	19.23	0.36	3	3		
92	498	-141	18.99	0.34	2	3		
93	494	-147	19.71	0.45	3	3		
94	496	-150	19.42	0.48	3	3		
95	485	-148	19.24	0.33	2	3		
96	479	-151	18.87	0.45	2	3		
			Region 7					
1	601	- 7	20.88	0.79	2	2		
2	605	- 13	21.36	0.32	2	2		
3	600	- 14	19.05	0.50	2	2		
4	610	- 18	20.37	0.62	2	2		
5	615	- 26	20.69	0.65	2	2		
6	605	- 29	16.31	0.92	3	2	83	
7	597	- 28	20.25	0.70	2	2		
8	591	- 23	19.69	0.57	2	2		
9	583	- 34	19.07	0.66	2	2		
10	593	- 35	17.54	0.42	2	2	82	
11	594	- 39	20.64	0.60	2	2		
12	593	- 43	20.44	0.66	2	2		
13	585	- 43	20.81	0.67	2	2		
14	580	- 44	20.52	0.56	2	2		
15	571	- 32	19.69	0.55	2	2		
16	568	- 36	20.61	0.65	2	2		
17	569	- 48	16.19	0.56	2	2	80	
18	562	- 51	20.97	0.56	2	2		
19	556	- 52	19.91	0.64	2	2		
20	551	- 78	18.46	0.83	2	2		
21	572	- 63	19.96	0.74	2	2		
22	567	- 78	20.12	0.84	2	2		
23	559	- 83	19.68	0.55	2	2		
24	558	- 87	17.72	0.75	2	2	118	
25	569	- 85	16.15	0.88	3	2	117	
26	577	- 78	18.93	0.69	2	2		
27	591	- 72	19.71	0.43	2	2		
28	606	- 67	13.66	1.42	2	2	95	41
29	590	- 60	19.36	0.55	2	2		
30	613	- 47	19.06	0.56	2	2		
31	606	- 39	18.75	0.59	2	2		
32	623	- 32	20.98	0.47	2	2		
33	632	- 38	20.67	0.93	2	2		
34	632	- 48	20.69	0.52	2	2		
35	618	- 62	20.06	0.47	2	2		
36	649	- 39	19.47	0.56	2	2		
37	652	- 42	20.55	0.81	2	2		
38	658	- 45	20.71	0.83	2	2		
39	664	- 50	20.71	0.93	2	2		
40	659	- 57	16.55	0.87	4	3	84	
41	649	- 53	19.42	0.54	2	2		
42	647	- 62	20.56	0.62	2	2		
43	669	- 68	19.57	0.53	2	2		
44	649	- 87	20.56	0.28	2	2		
45	649	- 89	20.33	0.61	2	2		
46	639	-104	16.23	0.58	2	2	100	
47	628	- 96	20.57	0.58	2	2		
48	621	- 88	19.48	0.54	2	2		
49	611	- 92	18.62	0.40	2	2		
50	610	-100	19.96	0.28	2	2		
51	616	-108	16.87	0.64	4	2	99	
52	613	-113	19.67	0.34	2	2		
53	614	-122	19.81	0.61	2	2		
54	599	-113	15.93	0.89	3	2	115	
55	591	-110	20.54	0.62	2	2		
56	583	-110	20.30	0.65	2	2		
57	584	-100	19.70	0.54	2	2		
58	580	-101	19.36	0.58	2	2		
59	572	- 99	20.01	0.48	2	2		
60	581	- 95	19.50	0.50	2	2		
61	579	- 91	20.53	0.40	2	2		
62	584	- 92	19.38	0.45	2	2		
63	592	- 91	19.53	0.56	2	2		
64	597	- 89	20.20	0.46	2	2		
65	598	- 92	19.84	0.42	2	2		
			Region 8					
1	809	- 44	13.15	0.75	2	2	90	51
2	821	- 17	17.18	0.75	3	3	89	
3	814	0	18.46	0.48	3	3		52
4	805	15	19.36	0.45	3	3		
5	799	1	20.87	0.63	2	3		
6	795	- 6	19.05	0.48	3	3		
7	769	- 13	20.16	0.63	3	2		
8	749	- 28	18.86	0.62	2	2		
9	745	- 42	20.78	0.47	3	2		
10	748	- 61	18.91	0.64	2	2		
11	782	- 44	20.60	0.78	3	3		
12	780	- 52	19.11	0.46	3	3		
13	780	- 57	17.09	0.75	3	2	91	
14	799	- 61	19.96	0.46	2	3		
15	817	- 62	20.08	0.63	3	2		
16	834	- 44	19.21	0.35	2	2		
17	834	- 60	20.76	0.51	2	3		
18	824	- 67	19.90	0.33	3	3		
19	818	- 84	17.02	0.80	3	3	92	
20	817	- 88	20.61	0.45	3	2		

Table 3–*continued*

Star	Δα	Δδ	V (mag)	B-V (mag)	N_v	N_b	Star number Stet-son	Fig. 1
			Region 9					
1	590	-233	19.75	0.64	2	3		
2	572	-233	19.29	0.45	3	3		
3	578	-239	19.56	0.46	3	3		
4	578	-241	20.30	0.80	2	2		
5	562	-247	18.00	0.73	3	3	166	
6	555	-241	19.50	0.69	3	3		
7	548	-260	17.06	0.83	3	3	167	
8	558	-266	19.11	0.52	3	3		
9	534	-265	20.22	0.41	2	2		
10	529	-262	19.67	0.48	2	2		
11	525	-264	20.10	0.49	3	2		
12	535	-272	20.20	0.43	3	2		
13	529	-274	19.59	0.46	2	2		
14	521	-271	19.46	0.44	3	2		
15	519	-271	20.27	0.75	2	2		
16	521	-274	19.73	0.50	3	2		
17	525	-276	17.45	0.75	4	3	171	
18	530	-283	16.24	0.86	2	3	172	
19	520	-292	19.08	0.44	3	3		
20	517	-281	19.69	0.41	3	2		
21	513	-279	19.48	0.42	2	3		
22	510	-286	19.54	0.51	2	3		
23	496	-278	19.64	0.50	2	3		
24	508	-271	19.22	0.44	2	2		
25	510	-265	20.31	0.48	2	2		
26	510	-262	19.37	0.48	2	2		
27	508	-259	19.24	0.45	2	2		
28	505	-258	19.44	0.42	3	2		
29	503	-269	17.58	0.77	4	2	170	
30	500	-267	19.49	0.29	3	2		
31	496	-265	18.78	0.66	3	3		
32	490	-271	20.19	0.38	3	3		
33	486	-267	19.74	0.45	3	2		
34	489	-264	19.96	0.50	2	2		
35	484	-260	20.21	0.34	3	2		
36	479	-261	19.54	0.52	3	3		
37	489	-253	20.06	0.44	3	2		
38	493	-250	20.04	0.52	3	2		
39	490	-248	19.18	0.43	3	3		
40	499	-244	19.72	0.59	2	3		
41	503	-244	19.03	0.44	2	3		
42	500	-254	19.98	0.49	2	2		
43	513	-252	19.37	0.48	3	3		
44	519	-253	19.54	0.44	2	3		
45	525	-256	19.61	0.49	2	2		
46	528	-254	20.55	0.57	2	2		
47	529	-248	18.81	0.64	3	3		
48	542	-245	19.74	0.44	3	3		
49	542	-242	19.50	0.46	3	3		
50	541	-237	19.14	0.52	3	3		
51	539	-231	16.48	0.86	5	4	165	
52	548	-230	19.43	0.49	3	3		
53	561	-233	20.40	0.62	3	2		
54	564	-227	20.86	0.55	3	2		
55	567	-224	20.25	0.36	3	3		
56	567	-215	19.85	0.51	3	2		
57	555	-203	19.43	0.43	3	3		
58	552	-207	20.69	0.66	2	2		
59	546	-205	20.47	0.56	3	2		
60	545	-201	20.65	0.43	2	2		
61	542	-205	20.33	0.73	2	3		
62	536	-209	19.74	0.42	3	2		
63	537	-213	20.27	0.66	2	2		
64	522	-217	14.38	1.20	2	2	164	35
65	537	-224	19.97	0.42	3	3		
66	543	-222	19.53	0.55	3	3		
67	512	-246	19.99	0.46	2	2		
68	519	-235	13.19	1.75	2	2	168	34
69	509	-231	20.17	0.21	2	2		
70	505	-235	18.83	0.62	3	3		
71	497	-231	19.67	0.53	3	2		
72	493	-232	19.18	0.42	2	2		
73	494	-234	20.20	0.59	3	3		
74	491	-234	19.70	0.45	2	3		
75	481	-243	19.66	0.59	2	3		
76	480	-244	19.73	0.21	2	3		
77	475	-246	19.82	0.67	3	2		
78	475	-255	19.57	0.41	2	2		
79	468	-254	19.74	0.55	2	2		
80	467	-251	19.88	0.55	2	2		
81	462	-253	19.48	0.28	3	2		
82	468	-247	18.78	0.65	3	3		
83	457	-249	19.84	0.49	3	3		
84	460	-246	20.36	0.40	3	2		
85	477	-237	16.23	0.94	2	2	169	
86	472	-236	19.37	0.42	2	2		
87	487	-229	19.21	0.38	2	3		
88	484	-228	20.49	0.59	3	2		
89	489	-226	19.47	0.25	3	2		
90	486	-222	16.91	0.03	3	3	162	
91	492	-221	18.93	0.52	2	2		
92	479	-222	20.62	0.55	2	2		
93	475	-226	19.51	0.45	3	2		
94	473	-221	18.66	0.54	2	2		
95	459	-231	18.14	0.61	3	3		
96	454	-221	18.98	0.50	2	2		
97	485	-215	16.24	0.79	2	2	161	
98	490	-212	20.10	0.52	2	2		
99	489	-210	19.97	0.49	2	2		
100	495	-215	19.68	0.63	3	3		
101	501	-213	17.74	0.74	2	3	163	
102	512	-210	19.45	0.47	3	3		
103	528	-198	20.09	0.58	3	3		
104	554	-199	19.61	0.31	2	3		
105	549	-195	19.65	0.51	3	2		
106	521	-190	20.50	0.49	3	2		
107	514	-184	18.25	0.71	3	3		
108	508	-190	19.87	0.43	3	2		
109	512	-194	19.73	0.46	2	2		
110	528	-184	17.72	0.74	3	3		
111	491	-201	17.81	0.68	2	3		
			Region 10					
1	441	-324	20.15	0.46	2	2		
2	433	-322	19.05	0.48	2	2		
3	434	-326	19.70	0.43	2	2		
4	418	-316	19.21	0.52	2	2		
5	415	-320	20.03	0.61	2	2		
6	412	-322	20.01	0.44	2	2		
7	416	-327	20.49	0.59	2	2		
8	413	-330	19.70	0.43	2	2		
9	409	-349	20.20	0.60	2	2		
10	389	-363	19.60	0.32	2	2		
11	382	-356	19.03	0.47	2	2		
12	390	-349	19.05	0.41	2	2		
13	381	-349	19.30	0.49	2	2		
14	375	-343	19.01	0.43	2	2		
15	373	-338	19.52	0.43	2	2		
16	377	-338	20.26	0.55	2	2		
17	398	-330	19.86	0.52	2	2		
18	391	-327	19.58	0.46	2	2		
19	396	-322	20.53	0.54	2	2		
20	405	-305	19.00	0.51	2	2		
21	400	-296	18.87	0.64	2	2		
22	382	-308	20.40	0.64	2	2		
23	377	-318	20.54	0.64	2	2		
24	375	-325	19.59	0.47	2	2		
25	367	-328	18.78	0.41	2	2		
26	366	-331	19.33	0.50	2	2		
27	358	-326	15.90	0.93	2	2	195	25
28	360	-332	20.67	0.58	2	2		
29	367	-338	20.51	0.65	2	2		
30	366	-344	20.08	0.47	2	2		
31	358	-342	20.59	0.40	2	2		
32	364	-352	18.61	0.67	2	2		
33	362	-356	20.52	0.45	2	2		
34	372	-359	19.15	0.32	2	2		
35	369	-361	19.67	0.50	2	2		
36	357	-372	19.61	0.44	2	2		
37	357	-367	20.24	0.54	2	2		
38	360	-361	20.74	0.67	2	2		
39	351	-353	19.94	0.56	2	2		
40	338	-373	20.48	0.54	2	2		
41	324	-357	18.69	0.60	2	2		
42	329	-354	20.51	0.44	2	2		
43	334	-350	19.27	0.46	2	2		
44	339	-344	19.98	0.51	2	2		
45	348	-337	20.32	0.42	2	2		
46	341	-337	19.55	0.47	2	2		
47	347	-330	20.58	0.47	2	2		
48	337	-330	19.63	0.50	2	2		
49	334	-324	19.50	0.42	2	2		
50	332	-327	19.32	0.41	2	2		
51	334	-338	20.03	0.49	2	2		
52	330	-339	19.85	0.46	2	2		
53	326	-339	19.46	0.37	2	2		
54	321	-338	18.81	0.58	2	2		
55	326	-334	19.70	0.33	2	2		
56	350	-365	20.08	0.52	2	2		
57	308	-348	19.56	0.45	2	2		
58	303	-348	19.08	0.36	2	2		
59	297	-331	19.46	0.37	2	2		
60	301	-330	19.53	0.41	2	2		
61	309	-324	19.68	0.37	2	2		
62	298	-324	19.07	0.53	2	2		
63	292	-327	19.95	0.42	2	2		
64	295	-321	19.44	0.46	2	2		
65	291	-319	20.43	0.57	2	2		
66	304	-318	20.43	0.48	2	2		
67	327	-313	16.47	0.89	2	2	196	
68	336	-309	19.46	0.42	2	2		
69	342	-309	19.03	0.33	2	2		
70	354	-313	19.42	0.33	2	2		
71	357	-314	20.09	0.37	2	2		
72	350	-320	20.09	0.42	2	2		
73	356	-306	20.46	0.74	2	2		
74	364	-303	19.57	0.62	2	2		
75	368	-301	17.19	0.78	2	2	199	26
76	382	-287	19.63	0.30	2	2		
77	377	-287	19.43	0.46	2	2		
78	378	-283	19.21	0.42	2	2		
79	324	-301	19.31	0.46	2	2		
80	340	-291	19.08	0.45	2	2		
81	328	-287	19.77	0.49	2	2		

data. The equations derived for the fit were:

$V = V_{eg} - 0.03(\pm 0.03)\ (B-V) - 2.79;$

$B = B_{eg} + 0.15(\pm 0.02)\ (B-V) - 2.14.$

Electronographic photometry possesses several important advantages over conventional photographic photometry, e.g. linearity of response, high detective quantum efficiency, high storage capacity and dynamic range, etc. However, Hawkins (1979) and Stewart (1979) found that there may sometimes be non-linearity in electronographic photometry. They found that this non-linearity occurred with film where a form of low density saturation was taking place, probably due to the lack of developable grains in a particular batch of nuclear emulsion. The problem was solved successfully following discussions with Ilford, the manufacturer, and using a system of quality checks at Royal Greenwich Observatory (*cf.* Hawkins 1981) and no further evidence for non-linearity has been found. The laboratory measurements by Kron, Ables & Hewitt (1969) and Kahan & Cohen (1969) as well as the direct comparisons of electronographic and photoelectric magnitudes by Walker & Kron (1967) and Penny (1976, 1984) have shown that the electronographic systems are linear over the expected range. The linearity of the present electronographic system has been confirmed by Hawkins (1981).

We used the *BV* magnitudes of stars measured from short exposures to tie the electronographic magnitudes measured on deep exposures into the standard *BV* system. The zero-point has been tied within an accuracy of ± 0.02 mag. Table 3 lists the difference in right ascension ($\Delta\alpha$) and declination ($\Delta\delta$) measured in arcsec with respect to star 3 in Fig. 1; the electronographic *BV* magnitudes and the number of measurements of each star. The positions were derived from a UK Schmidt Telescope photographic plate by tying in the (x, y) positions of the electronographic stars to SAO stars in the plate. The differential positions are accurate to 1 arcsec.

The internal accuracy, estimated from the scatter in the individual measures of different exposures, is $\sigma = 0.04$ mag, both in *B* and *V* passbands, for stars brighter than $V \approx 19$ mag and

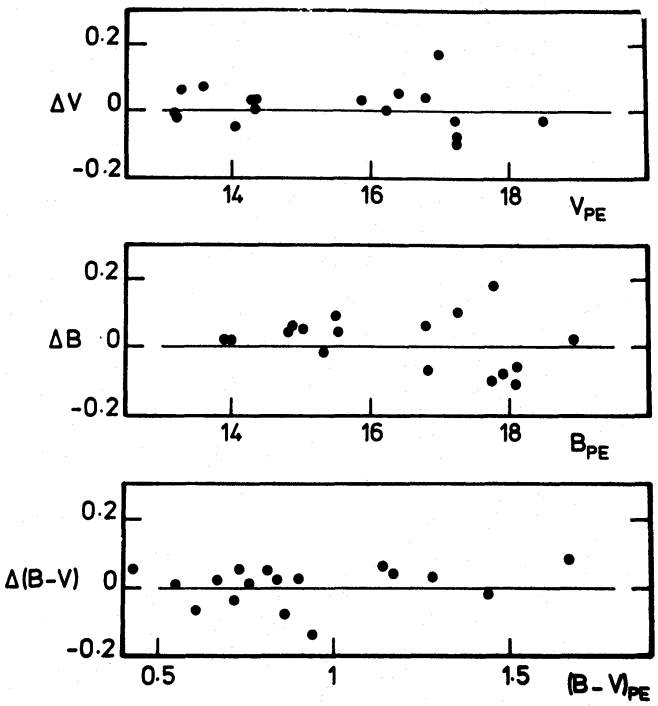

Figure 4. Comparison of photoelectric magnitudes with the electronographic ones. ΔV, ΔB and $\Delta(B-V)$ are the differences in the sense electronographic minus photoelectric.

increases for faint stars, becoming 0.07 mag both in B and V at $V \approx 21$ mag. Near the turn-off point, the error in $(B-V)$ is 0.10 mag, if one allows for the errors in the zero-point and colour coefficients of the transformation equation, but it increases for fainter stars and becomes ≈ 0.15 mag at the limit of observations. A comparison of present estimates with Stetson's (1981) photoelectric observations based on nine stars in the range of $V = 13.2$–16.5 mag gives standard deviations of ± 0.033 mag and ± 0.025 mag for ΔV and $\Delta(B-V)$ respectively, while the same with his photographic BV magnitudes based on 81 stars in the range of $V = 13.2$–17.8 mag yields $\Delta V = 0.02 \pm 0.08$ mag and $\Delta(B-V) = 0.00 \pm 0.08$ mag.

Apart from the stars used for deriving the colour equation, 17 stars in Table 3 have photoelectric BV magnitudes [see Table 1 and Stetson's (1981) photometry]. Fig. 4 compares photoelectric magnitudes with electronographic ones and confirms the linearity of the present electronographic system.

4 The colour–magnitude diagram

Fig. 5 shows the CMD for the cluster NGC 1851. In this diagram we have included the photographic data by Stetson (1981) because the present photoelectric and electronographic data have only a few stars brighter than $V = 17$ mag. The photoelectric and electronographic data are shown by large and small filled circles respectively, and the photographic data by open circles. Some of the brighter stars have been observed spectroscopically subsequently by us. These and Hesser *et al.* (1982) observations indicate that several have radial velocities incompatible with cluster membership. These stars are marked in Fig. 5. Overall there is good agreement between

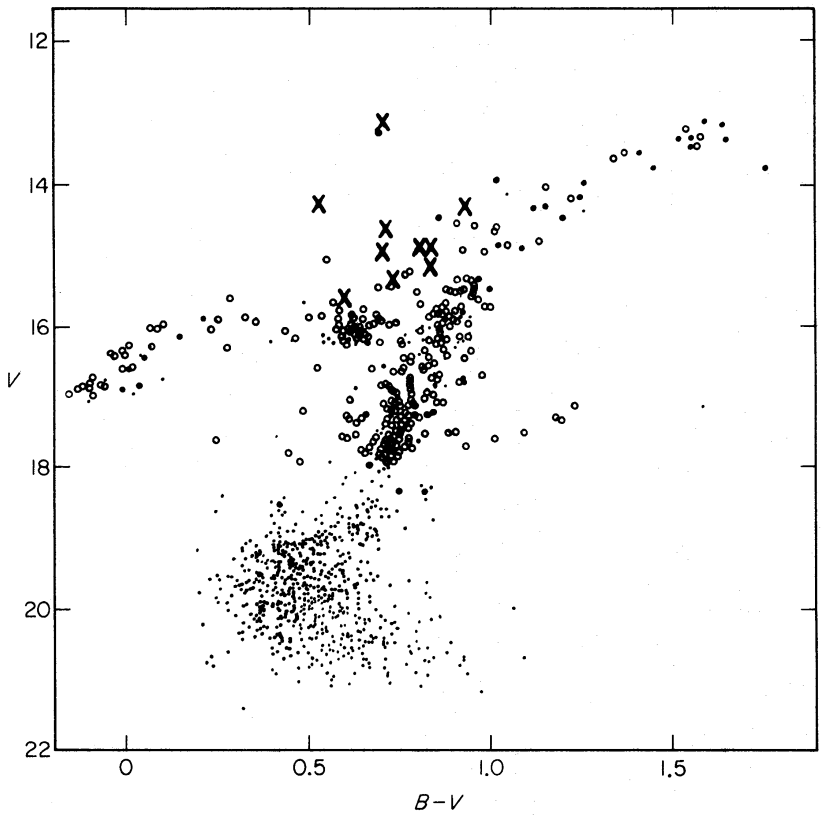

Figure 5. Colour–magnitude diagram for NGC 1851. Open circles represent the Stetson's (1981) photographic data. Large and small filled circles represent respectively the photoelectric and electronographic data. Stars having radial velocities incompatible with cluster membership are denoted by crosses.

the present photoelectric and electronographic data and the photographic data for the giant and subgiant branches, and towards the red end of the horizontal branch. However, the present observations of the blue end of the horizontal branch appear to be somewhat bluer than in Stetson's (1981) photgraphic data. It may be due to the fact that the photoelectric sequence used for calibrating the photographic observations has only very few stars in that region.

Recently Ratnatunga & Bahcall (1985) have predicted the number of field stars in the direction of NGC 1851. This has been used to estimate the number of field stars present in the CMD of the cluster. The electronographic observations are spread over ≈ 18 arcmin^2 while photographic observations (Stetson 1981) have been carried out in a radius of 6–7 arcmin with respect to the cluster centre. On this basis 20–25 field stars are expected for $V<17$ mag and 31 stars for $V\geqslant 17$. This constitutes a contamination of only 3 per cent, which is much too small to affect the conclusions of this paper.

We find the turn-off point (defined as the bluest point reached on the main sequence) to be at $(B-V)_t = 0.40\pm0.03$ mag, $V_t = 19.45\pm0.1$ mag. If we adopt $E(B-V)=0.02$ mag (Stetson 1981), we obtain $(B-V)_{0t}=0.38$ mag. The various CMD morphological parameters (Sandage 1982) that have been regarded as abundance indicators are:

$(B-V)_{0,g}=0.86\pm0.03$ mag;

$\Delta V=2.38$ mag;

$S=4.1$;

$\Delta V(\mathrm{TO-HB})=3.3\pm0.1$ mag.

These values are in good agreement with earlier estimates, for example $(B-V)_{0,g}=0.87\pm0.03$ mag, $\Delta V=2.4$ mag and $S=4.2$ given by Stetson (1981) and $\Delta V=2.5$ mag by Alcaino (1976). The apparent magnitude of the horizontal branch (HB), estimated directly from

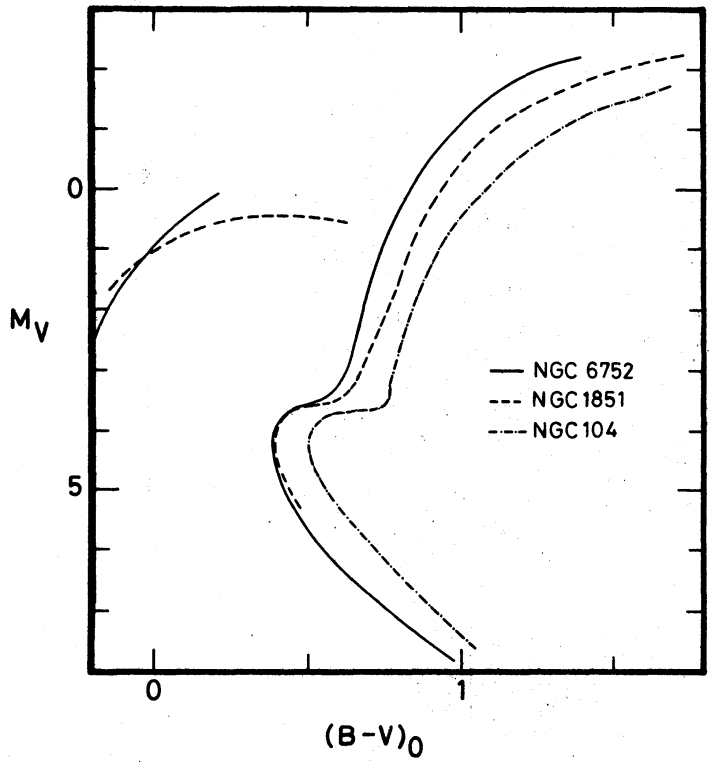

Figure 6. Comparison of the mean locus of NGC 1851 with other well studied globular clusters NGC 6752 and 104.

the plot yields $V_{HB} = 16.05 \pm 0.2$ mag. Assuming $M_V = 0.6$ mag for the HB, the apparent distance modulus $(m-M)$ is 15.45 ± 0.2 mag, which implies $(m-M)_0 = 15.39 \pm 0.3$ mag if we adopt $A_V = 0.06 \pm 0.04$ mag. The same value for the distance modulus has been found by Stetson (1981).

Recently, with the help of modern observing techniques, in particular using CCDs, accurate photometric observations down to the MS have become available for several galactic globular clusters. This makes possible comparison of the mean locus of the CMD of NGC 1851 with some of these well observed clusters. In Fig. 6, we compare the mean locus of the CMD of NGC 104 and 6752 with that of NGC 1851. The loci of NGC 104 and 6752 have been taken respectively from the CCD photometry by Penny & Dickens (1986) and Hesser *et al.* (1987). For these clusters, the distance moduli and $E(B-V)$ values used for deriving M_V and $(B-V)_0$ are also taken from the same work. Overall the location of the mean locus of the cluster NGC 1851 lies between those of NGC 104 and 6752 as expected from the different metallicities quoted in Section 2.

For cluster age estimation, VandenBerg & Bell (1985) theoretical isochrones have been used. Most of the studies which have used these isochrones to fit new CCD data for globular clusters (*cf.* Hesser *et al.* 1987 and references therein) have found it necessary to shift the theoretical loci by $\delta(B-V) = 0.03$ mag in the redward direction in order to obtain the best match to the data. VandenBerg (1986) has also mentioned that more likely the predicted temperatures of the

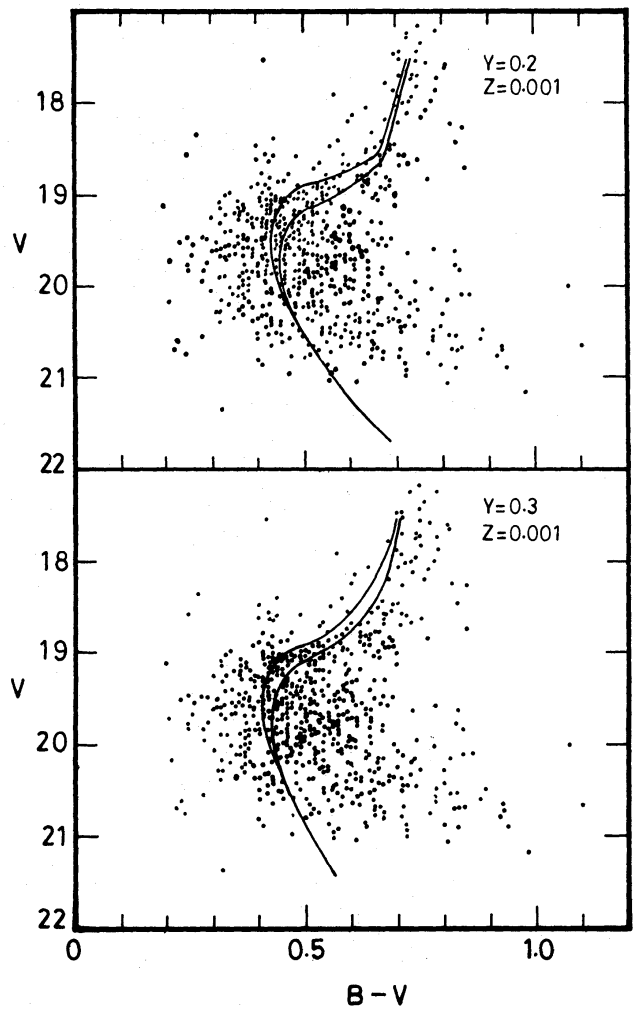

Figure 7. The main-sequence and subgiant portion of the colour–magnitude diagram overlaid by the best-fitted VandenBerg & Bell (1985) isochrones for $Y = 0.3$, $z = 0.001$ and $Y = 0.2$, $z = 0.001$. For each composition, isochrones for ages of 14×10^9 and 16×10^9 yr are shown, where the younger age is the brighter and bluer.

models are hot and suggests a similar correction. Hence, we have also applied this correction to the VandenBerg & Bell (1985) isochrones and then fitted to the data by eye, in the region of the turn-off point and subgiant branch for different values of Y and age. There seems to be a small discrepancy between the best-fit isochrone and the data near the sample limit, and only observations to a fainter limit can clarify the situation. Clearly NGC 1851 would be a good target now for high-precision faint star photometry using a CCD camera. The best fit isochrones are shown in Fig. 7. Diagrams for two different values of Y are given, and that with $Y=0.2$ appears to be the best fit to the observations. On this basis an age of 15 ± 3 Gyr is estimated for the cluster NGC 1851. This is identical, within the error, to most recently derived ages of other globular clusters based on the same set of theoretical isochrones (*cf.* Hesser *et al.* 1987; VandenBerg 1986 and references therein).

5 Conclusions

Present analysis leads to the following conclusions:

(i) The present CMD extends previous observations to about 2 mag below the turn-off point.

(ii) The overall shape of the CMD is consistent with the intermediate metallicity of the cluster and agrees with the VandenBerg & Bell (1985) theoretical isochrone for $z=0.001$, $Y=0.2$ and the appropriate cluster age.

(iii) Comparison with theoretical isochrones gives an age of 15 ± 3 Gyr, which is in good agreement with the ages given for other well studied galactic globular clusters (Peterson 1986). In addition to this, the difference between the luminosities of the horizontal branch and turn-off point for NGC 1851 is 3.3 ± 0.1 mag, a value very close to the 3.4 mag found by Sandage (1982) and Peterson (1986) for several other clusters. In this light, we can conclude that the present work supports the classical dynamical model of our Galaxy proposed by Eggen *et al.* (1962) and, on the basis of this age estimate, that the Hubble constant cannot be higher than about 60 km s^{-1} Mpc^{-1}.

Acknowledgments

The authors express their thanks to Dr C. D. Pike and Dr A. J. Penny for their help and valuable suggestions during the scanning of the electronographic film at RGO and also later on during the reduction. One of us (RS) thanks the Royal Society of London for providing financial support through the Nuffield Foundation. Help from and discussions with Dr P. J. Godwin are also gratefully acknowledged.

References

Alcaino, G., 1969. *Astrophys. J.*, **156,** 853.
Alcaino, G., 1971. *Astr. Astrophys.*, **15,** 360.
Alcaino, G., 1976. *Astr. Astrophys.*, **50,** 299.
Cannon, R. D., 1981. *Mon. Not. R. astr. Soc.*, **195,** 1.
Cannon, R. D. & Stobie, R. S., 1973. *Mon. Not. R. astr. Soc.*, **162,** 207.
Cousins, A. W. J., 1973. *Mem. R. astr. Soc.*, **77,** 223.
Eggen, O. J., Lynden-Bell, D. & Sandage, A., 1962. *Astrophys. J.*, **136,** 748.
Harris, W. E. & Racine, R., 1979. *Ann. Rev. Astr. Astrophys.*, **17,** 241.
Hawkins, M. R. S., 1979. *Mon. Not. R. astr. Soc.*, **188,** 691.
Hawkins, M. R. S., 1981. *Mon. Not. R. astr. Soc.*, **194,** 1013.
Hesser, J. E., Bell, R. A., Cannon, R. D. & Harris, G. L., 1982. *Astr. J.*, **87,** 1470.
Hesser, J. E., Harris, W. E., VandenBerg, D. A., Allwright, J. W. B., Shott, P. & Stetson, P., 1987. *Publs astr. Soc. Pacif.* (submitted).
Kahan, E. & Cohen, M., 1969. *Adv. Electronics Electron Phys.*, **28B,** 725.

Kinman, T. D., 1959. *Mon. Not. R. astr. Soc.,* **119,** 538.
Kron, G. E., Ables, H. D. & Hewitt, A. V., 1969. *Adv. Electronics Electron Phys.,* **28A,** 1.
Liller, M. H., 1975. *Astrophys. J.,* **201,** L125.
Penny, A. J., 1976. *PhD thesis,* University of Sussex.
Penny, A. J., 1984. *Mon. Not. R. astr. Soc.,* **208,** 559.
Penny, A. J. & Dickens, R. J., 1986. *Mon. Not. R. astr. Soc.,* **220,** 845.
Peterson, C. J., 1986. *Publs astr. Soc. Pacif.,* **98,** 1258.
Ratnatunga, K. U. & Bahcall, J. N., 1985. *Astrophys. J. Suppl.,* **59,** 63.
Sandage, A., 1982. *Astrophys. J.,* **252,** 553.
Searle, L. & Zinn, R., 1978. *Astrophys. J.,* **225,** 357.
Stetson, P. B., 1981. *Astr. J.,* **86,** 687.
Stewart, N. J., 1979. *PhD thesis,* University of Edinburgh.
VandenBerg, D. A., 1986. *Mem. Soc. astr. Ital.,* **57,** 373.
VandenBerg, D. A. & Bell, R. A., 1985. *Astrophys. J. Suppl.,* **58,** 561.
Walker, M. F. & Kron, G. E., 1967. *Publs astr. Soc. Pacif.,* **79,** 551.
Wehlau, A., Liller, M. H., Clement, C. C. & Wizinowich, P., 1982. *Astr. J.,* **87,** 295.
Wehlau, A., Liller, M. H., Demers, S. & Clement, C. C., 1978. *Astr. J.,* **83,** 598.
Zinn, R. & West, M. J., 1984. *Astrophys. J. Suppl.,* **55,** 45.